To be submitted to 1997 International Conference on Robotics and Automation

On 3D Vision Based Active Antenna

Naoki Kanayama Makoto Kaneko Toshio Tsuji
Industrial and Systems Engineering
Hiroshima University
Kagamiyama Higashi-Hiroshima 739, Japan

Abstract

This paper discusses the 3D Vision Based Active Antenna (3D-VBAA) that can detect the contact force and the contact point between an insensitive elastic antenna and a 3D environment. The 3D-VBAA is composed of an insensitive flexible antenna, two actuators, two position sensors, a camera, and a one-axis moment sensor. By utilizing the antenna's shape mapped into the calibration plane C, the vision sensor can provide both the contact distance and a force component on C. The moment sensor output allows us to evaluate the force component normal to C. The 3D-VBAA can work even under a compliant object, while the 3D Active Antenna [1] can not. We show that the coupling effect between vision and moment sensor depends on the implementation angle of the CCD camera. We verify our idea experimentally.

1 Introduction

There have been a number of works discussing whisker-like sensors. A simple flexible beam sensor can take the form of a short length of spring piano wire or hypodermic tubing anchored at the end. When the free end touches an external object, the wire bends. This can be sensed by a piezoelectric element or by a simple switch [2]. A more elaborate sensor is described by Wang and Will [3]. Long antennae-like whisker sensors were mounted on the SRI mobile robot, Shakey [4], and on Rodney Brook's six-legged robot insects [5]. Hirose, et.al. discussed the utilization of whisker sensors in legged robots [6]. Similarly shaped whiskers have been considered for the legs of the Ohio State University active suspension vehicle [7]. The major difference between previous works [2]–[7] and ours is that the VBAA can detect the contact point between the antenna and the environment, while previous works do not.

There are several works combining both tactile and vision sensors to take advantage of each sensor. For example, Stansfield presented a robotic perceptual system which utilizes passive vision and active touch [8]. Allen proposed an object recognition system that uses passive stereo vision and active exploratory tactile sensing [9]. These works utilized two different kinds of sensors to increase sensing capability.

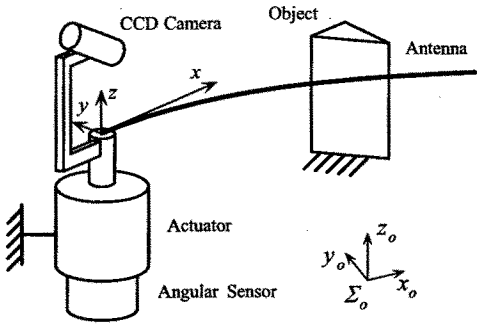

Fig.1 An overview of 2D-VBAA.

In our former work, we have shown that if the environment is rigid, the contact location is a function of the rotational compliance of the antenna in contact with the environment, and that it can be obtained by utilizing the outputs from both joint position and torque sensors. Such a sensing system has been termed the Active Antenna [10, 11, 12]. This idea has also been extended to a 3D version [13, 14]. Ueno and Kaneko discussed the Dynamic Active Antenna, in which the contact location is estimated through the measurement of natural frequency of a flexible beam whose dynamics is changed according to the contact location between the environment and itself [15, 16]. A big advantage of the Active Antenna is that a location of the contact point is obtained through a surprisingly simple active motion, while sophisticated active motions should be prepared in most contact sensing methods in order to avoid large interaction force between the sensor and the environment. This is because the flexibility of the antenna itself successfully relaxes the contact force, even under a large positional error.

However, the Active Antenna cannot work appropriately in a compliant environment, since the sensor system is not able to break down the measured compliance into that coming from the antenna itself and that coming from the environment. The difficulty of decomposition comes from the sensor system utilizing only local information, such as the joint torque and the joint angular displacement, but not taking any global information into consideration. This is the reason why a vision system is introduced into the VBAA. The VBAA allows us to detect the contact location even under a compliant environment. We first considered the basic working principle for the 2D-VBAA, as

shown in Fig.1. The camera continuously observes the antenna's shape during an active motion imparted to the antenna. By observing the shape distortion from it's original straight line position, the sensor system can detect any initial contact with the environment. With a further active motion, the antenna deforms according to the pushing angle, the contact location, and the environment's stiffness. The pushing angle can be regarded as input for the 2D-VBAA, and the antenna's shape obtained through the CCD camera can be regarded as the output. By analyzing proceeding the input-output relationship, the 2D-VBAA can detect the contact distance, the contact force, and the environment's stiffness. We would emphasize that the vision is not used to detect the contact point directly but used to observe the antenna's shape. Because of this feature, the 2D-VBAA can detect both contact location and contact force even though the exact contact point is hidden by occlusion. However, so far we implicitly assume that the antenna's deformation is restricted to the calibration plane $\mathcal{C}$ and never away from the plane.

In this paper, we propose the 3D-VBAA which can work in a 3D environment. One emphasis of our work is that we obtain the contact position and the contact force by fusing both visual and moment information. The visual information is utilized for obtaining the contact distance and one component of the contact force. One interesting result is that even when a part of antenna is away from $\mathcal{C}$ due to the environment geometry, we can evaluate both contact distance and one force component from the antenna's shape projected on $\mathcal{C}$. The moment sensor is utilized to compensate for the information that can not be obtained by vision sensor. The force component perpendicular to $\mathcal{C}$ can be obtained by the moment sensor including the force component perpendicular to $\mathcal{C}$. We find that the orthogonal arrangement between vision and moment sensors contributes to reducing the coupling effect between two sensors. We show that the 3D-VBAA can provide both the contact position and the contact force except the axial component, even under a compliant environment, while the previous 3D Active Antenna can not. We also show some experimental results to verify the basic working principle of the proposed 3D-VBAA.

2 3D-VBAA

The 2D-VBAA can only work under the condition that a column object is placed perpendicular to the motion plane of the antenna as shown in Fig.1. This assumption ensures that the antenna never makes slip in the lateral direction, while a longitudinal slip inevitably occurs to satisfy the geometrical condition before and after a bending deformation. We now remove this assumption and allow the beam to make a slip not only in the longitudinal but also in the lateral directions. We begin by describing the main assumptions in section 2.1.

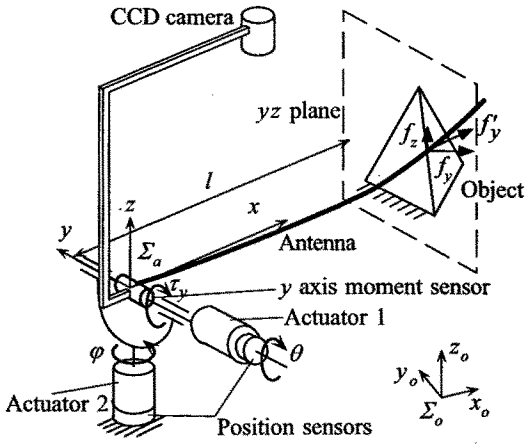

Fig.2 Basic structure of the 3D-VBAA.

2.1 Main Assumptions

Main assumptions taken here are as follows:

Assumption 1: The deformation of the antenna is small enough to ensure that the antenna's behavior obeys the force-deformation relationship obtained by linear theory.

Assumption 2: The environment (or the object) to be sensed is stationary during the active motions.

Assumption 3: All pixels concerning the antenna are already extracted from the scene.

Assumption 4: The antenna has equal compliance in the place perpendicular to the longitudinal axis.

2.2 Basic structure of 3D-VBAA

In the 3D-VBAA, we implement one moment sensor in addition to a vision sensor. The vision sensor can incorporate the antenna's shape projected on the calibration plane $\mathcal{C}$ where $\mathcal{C}$ is defined by the plane xy as shown in Fig.2. But it includes no information on the antenna shape projected on the plane perpendicular to the vision axis. In order to obtain the information on the antenna shape projected on the plane perpendicular to $\mathcal{C}$, we implement a moment sensor. As a result, the 3D-VBAA is composed of one flexible antenna, two actuators for moving the antenna in 3D space, two angular sensors for detecting the position, one-axis moment sensor, and a CCD camera to observe the shape of antenna as shown in Fig.2. The camera is fixed on the attachment whose base is moved by the actuator. Therefore, the camera can rotate with the antenna.

2.3 Working principle

Figure 3 shows the antenna shape after a pushing motion is imparted to the antenna in contact with 3D object. By assumption 4, both the contact force and the antenna displacement should lie on the $x'y'$ plane (Deformation plane $\mathcal{D}$). The camera can take in the

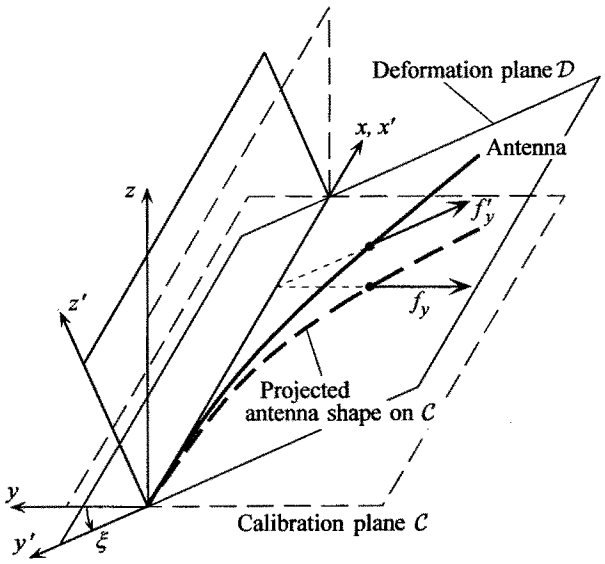

Fig.3 Projection of the antenna shape to xy plane.

antenna shape mapped into $\mathcal{C}$. Figure 4 shows the antenna deformation on $\mathcal{D}$. In $\mathcal{D}$, the antenna shape is given by

Curved Part $(0 < x \leq l \leq L)$,

$$y' = \frac{f'_y}{6EI}(3l - x')x'^2 . \tag{1}$$

Straight-Lined Part $(0 < l \leq x \leq L)$,

$$y' = \frac{f'_y}{6EI}(3x' - l)l^2 , \tag{2}$$

where (x', y'), l, L, E and I denote a point on the antenna, the contact distance, the length of the antenna, Young's modulus of the antenna and the second order moment of the cross section of the antenna, respectively. The antenna shape is mapped from $\mathcal{D}$ to $\mathcal{C}$ by the transformation $\boldsymbol{T}$.

$$\boldsymbol{T} = \begin{bmatrix} 1 & 0 \\ 0 & \cos\xi \end{bmatrix} \tag{3}$$

where ξ is the angle between y' and y axes, and a vector $\boldsymbol{x}' = (x', y')^t$ is transformed in $\boldsymbol{x} = (x, y)^t$ by $\boldsymbol{x} = \boldsymbol{T}\boldsymbol{x}'$.

By the transformation $\boldsymbol{T}$, $x = x'$ and $y = y' \cos\xi$. Also, the contact force is simply mapped into $f_y = f'_y \cos\xi$. By substituting x', y' and f'_y into eqs.(1) and (2), we can obtain

$$\frac{y}{\cos\xi} = \frac{f_y}{6EI\cos\xi}(3l - x)x^2 \text{ (curved part)}, \tag{4}$$

$$\frac{y}{\cos\xi} = \frac{f_y}{6EI\cos\xi}(3x - l)l^2 \text{ (straight-lined part)}. \tag{5}$$

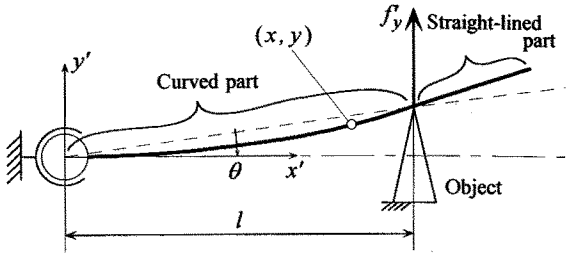

Fig.4 Antenna shape on $\mathcal{D}$.

From eqs.(4) and (5), we can obtain the following relationship

$$y = \frac{f_y}{6EI}(3l - x)x^2 \text{ (curved part)}, \tag{6}$$

$$y = \frac{f_y}{6EI}(3x - l)l^2 \text{ (straight-lined part)}. \tag{7}$$

Equations (6) and (7) mean that even if the antenna deforms in z direction, the force-deformation relationship in $\mathcal{C}$ is similar to that obtained for the 2D-VBAA. This is noticeable because we can estimate both the contact distance l and the y directional force component f_y by the vision data alone if $\xi \neq \pi/2$.

In eqs. (6) and (7), unknown parameters are f_y and l. So, the antenna shape is uniquely determined if f_y and l are given. The deformed antenna has curved part and straight-lined part. When we get two points on the antenna, there are three combination of points, namely, two points from the curved part, two points from the straight-lined part, and points from each of the curved and straight-lined part.

(i) Two points from the curved part

From eq.(6), we can obtain the following two equations.

$$y_1 = \frac{f_y}{6EI}(3l - x_1)x_1^2 , \tag{8}$$

$$y_2 = \frac{f_y}{6EI}(3l - x_2)x_2^2 , \tag{9}$$

where l should satisfy the condition of $0 < x_1 < x_2 \leq l$. From eq.(8) and (9), we can easily show the unique set of solutions in $0 < x_1 < x_2 \leq l$ as follows,

$$f_y = 6EI\frac{x_2^2 y_1 - x_1^2 y_2}{x_1^2 x_2^2 (x_2 - x_1)}, \tag{10}$$

$$l = \frac{x_1^3 y_2 - x_2^3 y_1}{3(x_1^2 y_2 - x_2^2 y_1)} . \tag{11}$$

Note that $x_2 - x_1 \neq 0$, $x_1^2 y_2 - x_2^2 y_1 \neq 0$, $x_1 \neq 0$, $x_2 \neq 0$ under $0 < x_1 < x_2 \leq l$.

(ii) Two points from the straight-lined part

In this case, we can obtain the following two equations.

$$y_1 = \frac{f_y}{6EI}(3x_1 - l)l^2, \quad (12)$$

$$y_2 = \frac{f_y}{6EI}(3x_2 - l)l^2, \quad (13)$$

where l should satisfy the condition of $0 < l \leq x_1 < x_2$. From eq.(12) and (13), we can introduce the unique set of solutions in $0 < l \leq x_1 < x_2$ as follows,

$$f_y = 2EI\frac{-(y_1 - y_2)^3}{9(x_2 - x_1)(x_1y_2 - x_2y_1)}, \quad (14)$$

$$l = \frac{3(x_1y_2 - x_2y_1)}{y_2 - y_1}. \quad (15)$$

Note that $x_2 - x_1 \neq 0$, $y_2 - y_1 \neq 0$, $x_1y_2 - x_2y_1 \neq 0$ under $0 < l \leq x_1 < x_2$.

(iii) Points from each of the curved and straight-lined parts

We omit the complete form of the solution due to the paper space limitation. Our previous work proves that there exists the unique pair of contact distance and contact force [17].

Once the contact distance is determined by the visual data, the z-directional force component can be evaluated by the moment sensor output. Since $\tau_y = lf_z$,

$$f_z = \frac{\tau_y}{l} \quad (16)$$

By utilizing f_y and f_z, we can estimate the antenna displacement at the contact point as follows,

$$\Delta y = \frac{f_y l^3}{3EI}, \quad (17)$$

$$\Delta z = \frac{f_z l^3}{3EI}, \quad (18)$$

where Δy and Δz denote the antenna displacements after it makes contact with the object. By estimating Δy and Δz, we can obtain the current contact point which differs from the initial one. We note that l, f_y, f_z, Δy and Δz can be evaluated irrespective of the object's compliance, while the 3D Active Antenna cannot work under a compliant object.

By using l, Δy and Δz, we can obtain the contact position with respect to the absolute coordinate system Σ_o. The contact point in Σ_o is given by

$$\boldsymbol{x}_a^{(o)} = \boldsymbol{x}_0^{(o)} + \boldsymbol{R}_a^o \boldsymbol{x}_a^{(a)} \quad (19)$$

$$\boldsymbol{x}_a^{(a)} = (l, \Delta y, \Delta z)^t \quad (20)$$

$$\boldsymbol{x}_0^{(o)} = (x_0, y_0, z_0)^t \quad (21)$$

$$\boldsymbol{R}_a^o = \begin{bmatrix} \cos\theta\cos\varphi & -\sin\varphi & -\sin\theta \\ \cos\theta\sin\varphi & \cos\varphi & 0 \\ \sin\theta & 0 & \cos\theta \end{bmatrix} \quad (22)$$

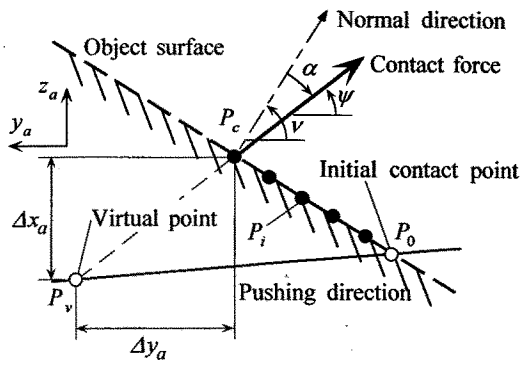

Fig.5 Detecting normal direction.

where θ and φ are angles for actuator 1 and 2, respectively, and the superscript (o) and (a) denote the values with respect to Σ_o and Σ_a, respectively and $\boldsymbol{R}_a^o$ is the rotational matrix from Σ_a to Σ_o. We note that the 3D-VBAA can continuously provide the contact point even during a lateral slip, while the conventional 3D-Active Antenna [1] can not. By making use of this property, we can obtain the local shape of object by connecting each contact point continuously.

Since the 3D-VBAA can provide both f_y and f_z, we can evaluate the direction of contact force projected on yz plane. By combining both the force and the local shape information, we can also estimate the frictional coefficient at the point of contact. Figure 5 explains an example, where the contact force is mapped into yz plane. To simplify the discussion, we assume that a knife edge like object is placed perpendicular to the antenna axis. Let P_i $(i = 0, 1, \ldots)$ be contact point. The antenna starts to deform when it comes to P_0. Each contact point P_i can be computed by the proposed method. By simply connecting each detected point, we can reconstruct the object shape as shown in Fig.5, and the normal direction ν can be estimated from the object shape. From two force components f_y and f_z, we can compute the direction ψ of the contact force projected on yz plane. As a result, we can evaluate the top angle of the friction cone $\alpha = \tan^{-1}\mu$, where μ is the friction coefficient at the point of contact. Thus, the 3D-VBAA enables us to obtain not only the contact position $\boldsymbol{x}_a^{(a)} = (l, \Delta y, \Delta z)^t$ but also the frictional coefficient at the point of contact.

3 Experiments

Figure 6 shows the overview of experimental setup, where a knife-edge like object is used. Instead of mounting the camera on the shaft of the actuator, we fix it in the base as shown in Fig.6 and the object is moved to obtain an equivalent effect. In order to suppress the frictional effect, we use extremely slippery objects and also impart an appropriate vibration to the antenna to reduce the frictional effect only when it makes contact with the object. The image data are

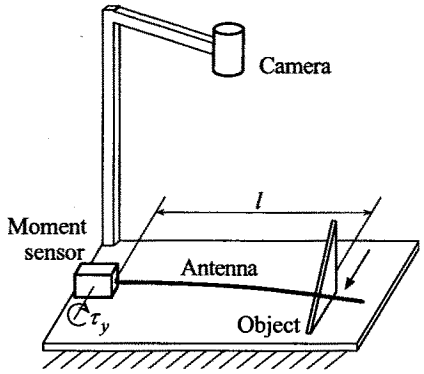

Fig.6 An overview of the experimental device.

fed into the computer through a CCD camera with 512 × 512 dots and 8bits gray scale. For easily distinguishing the antenna from the environment, we use a white stainless antenna with a diameter of 0.8mm and a length of 240mm. We believe that one of the big advantage of VBAA is that we can paint the antenna so that it may be easily distinguished from the environment.

Figure 7 shows experimental results where (a) and (b) show the estimated contact distance and the estimated contact force direction, respectively. For this experiment, three objects with different normal direction are used. As shown in Fig.7(a), the estimation of contact distance can be executed with high accuracy, even though the contact points do not exist on C. It can be seen from Fig.7(b) that the estimated direction of contact force almost coincides with that of normal direction of object's surface. This is because the frictional effect is reduced as much as possible in the experiment.

4 Discussions

In this work, we implicitly assume that the camera is implemented so that its axis is perpendicular to xy plane as shown in Fig.8 (see camera A). For actual application, such sensor configuration occupies a large sensor space and increases the moment of inertia around the actuator shaft, which is not desirable from the viewpoint of the compact design of the sensor system and for quickly rotating both the antenna and the camera. To cope with this problem, we consider to implement the camera with inclination angle ϕ as shown in Fig.8 (see camera B). In such a case, the antenna shapes projected on the C vary according to the camera position and angle. For example, let us consider an arbitrary point $\boldsymbol{p} = (x, y, z)^t$ on the antenna with the inclination angle ϕ as shown in Fig.8. An arbitrary point $\boldsymbol{p}$ is projected on C by each camera in such a way that

$$\boldsymbol{p}_A = (x, y, 0)^t \quad (23)$$

$$\boldsymbol{p}_B = (x + z\tan\phi, y, 0)^t \quad (24)$$

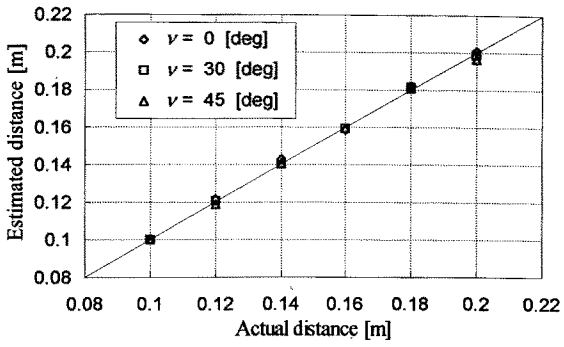

(a) Estimated distance

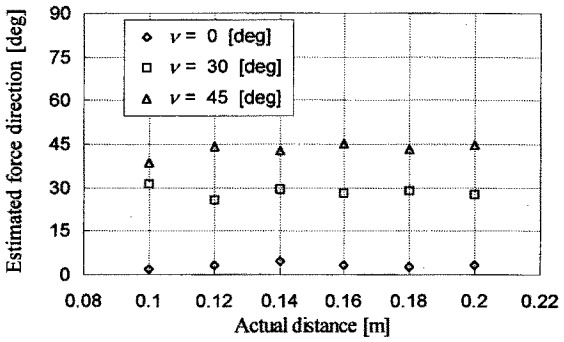

(b) Estimated force direction

Fig.7 Experimental results about 3D object sensing.

Therefore, if $\phi \neq 0$, $\boldsymbol{p}_B$ is not equal to $\boldsymbol{p}_A$. This means that the antenna shape no longer obeys according to the basic equations (6) and (7). In order to obtain the contact distance under $\phi \neq 0$, let us first formulate how a point on the antenna is mapped on C. Suppose that an arbitrary point $\boldsymbol{x}^{(a)} = (x, y, 0)^t$ on the antenna is mapped to $\boldsymbol{x}^{(a)} = (x_p, y_p, 0)^t$ on C, where . x_p and y_p are measured by the camera and given by

$$\begin{pmatrix} x_p \\ y_p \\ 0 \end{pmatrix} = \begin{pmatrix} x + \frac{\tau_y}{6EI}(3x - l)l\tan\phi \\ y \\ 0 \end{pmatrix}. \quad (25)$$

From eq.(25), we can express $\boldsymbol{x}^{(a)} = (x, y, 0)^t$ by using $\boldsymbol{x}^{(a)} = (x_p, y_p, 0)^t$ as follows:

$$\begin{pmatrix} x \\ y \\ 0 \end{pmatrix} = \begin{pmatrix} \frac{2EIx_p + \tau_y\tan\phi l^2}{2EI + \tau_y\tan\phi l} \\ y_p \\ 0 \end{pmatrix}. \quad (26)$$

where z is replaced by

$$z = \frac{f_z}{6EI}(3x - l)l^2 \quad (27)$$

$$= \frac{\tau_y}{6EI}(3x - l)l. \quad (28)$$

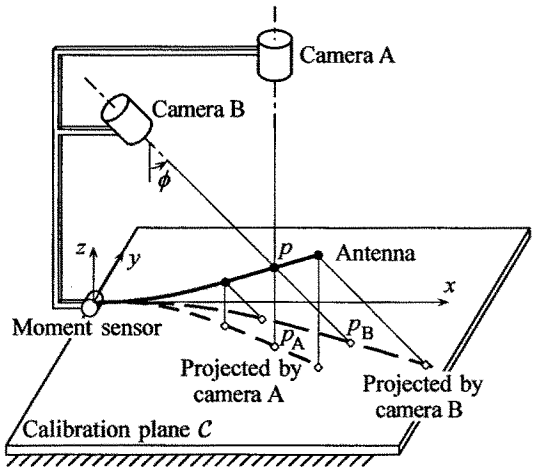

Fig.8 The projected images depending on ϕ.

where τ_y is measured by the moment sensor. Therefore, as far as $\phi \neq 0$, the vision and the moment sensor output are coupled each other. Since $(x, y, 0)^t$ in eq.(26) exists on the antenna shape equivalently projected by camera A, the relationship between x and y should obeys to eqs.(6) or (7). Therefore, for two arbitrary points $(x_{p1}, y_{p1}, 0)^t$ and $(x_{p2}, y_{p2}, 0)^t$ on C, we can obtain the following equations for computing the contact distance l.

(i) Two points from the curved part

By substituting x_{pi} and y_{pi} $(i = 1, 2)$ in eq.(26) into eq.(11), we can obtain the following equation

$$\begin{aligned} &8\gamma^3(y_{p2} - y_{p1})l^6 + 3\gamma^2(y_{p2} - y_{p1})l^5 \\ &+ 15\gamma^2(x_{p1}y_{p2} - x_{p2}y_{p1})l^4 + 6\gamma(x_{p1}y_{p2} - x_{p2}y_{p1})l^3 \\ &+ 6\gamma(x_{p1}^2 y_{p2} - x_{p2}^2 y_{p1})l^2 + 3(x_{p1}^2 y_{p2} - x_{p2}^2 y_{p1})l \\ &- (x_{p1}^3 y_{p2} - x_{p2}^3 y_{p1}) = 0 \end{aligned} \tag{29}$$

where $\gamma = \tau_y \tan\phi / 2EI$. Of cause, if $\phi = 0$, eq.(29) results in eq.(11). In case of $\phi \neq 0$, we have to solve 6-th order polynomial equation for obtaining l which may require rather tough computation task. Another remark is that we need the moment information τ_y to solve eq.(29), which means that both vision and moment sensor outputs are highly coupled each other, under $\phi \neq 0$.

(ii) Two points from the straight-lined part

By substituting x_{pi} and y_{pi} $(i = 1, 2)$ in eq.(26) into eq.(15), we can obtain

$$l = \frac{3(x_{p1}y_{p2} - x_{p2}y_{p1})}{y_{p2} - y_{p1}} \tag{30}$$

We note that l has the exactly similar form to that in $\phi = 0$. Equation (30) means that we can compute the contact distance as if we utilized the camera with $\phi = 0$. This result suggest that we should use the date close to the antenna tip so that we can make the most advantage of the straight-lined part.

(iii) Points from each of the curved and straight-lined parts

We again omit the complete form of the solution due to the paper space limitation.

5 Conclusion

By utilizing the technique of sensor fusion between a vision and a moment sensor, we proposed the 3D-VBAA which can detect the contact point in 3D space and the contact force except the axial component. We explained the basic working principle and showed some experimental results to verify the idea. We further considered how to design the compact sensor and how to reduce the moment of inertia of the system.

References

[1] Kaneko, M., N. Kanayama, and T. Tsuji: Vision Based Active Antenna, *1996 IEEE Int. Conf. on Robotics and Automation*, pp2555–2560, 1996.

[2] Russell, R. A.: Closing the sensor-computer-robot control loop, *Robotics Age*, April, pp15–20, 1984.

[3] Wang, S. S. M., and P. M. Will: Sensors for computer controlled mechanical assembly, *The Industrial Robot*, March, pp9–18, 1978.

[4] McKerrow, P.: Introduction to Robotics, *Addison-Wesley*, 1990.

[5] Brooks, R. A.: A robot that walks; Emergent behaviors from a carefully evolved network, *Neural Computation*, vol.1, pp253–262, 1989.

[6] Hirose, S., et.al.: Titan III: A quadrupled walking vehicle, *Proc. of the Second Int. Symp. on Robotics Research*, MIT Press, Cambridge, Massachusetts, 1985.

[7] Schiebel, E. N., H. R. Busby, K. J. Waldron: Design of a mechanical proximity sensor, *Robotica*, vol.4, pp221–227, 1986.

[8] Stansfield, S. A: A robot perceptual system utilizing passive vision and active touch, *The International Journal of Robotics Research*, vol.7, no.6, pp138–161, 1988.

[9] Allen, P. K.: Integrating vision and touch for objects recognition tasks, *The International Journal of Robotics Research*, vol.7, no.6, pp15–33, 1988.

[10] Kaneko, M: Active Antenna, *Proc. of the 1994 IEEE Int. Conf. on Robotics and Automation*, pp2665–2671, 1994.

[11] Kaneko, M., N. Ueno, and T. Tsuji: Active Antenna (Basic Working Principle), *Proc. of the 1994 IEEE Int. Conf. on Intelligent Robotics and Systems*, pp1744–1750, 1994.

[12] Kaneko, M., N. Kanayama, and T. Tsuji: A New Consideration on Active Antenna, *Proc. of the 1995 IEEE/RSJ Int. Conf. on Intelligent Robots and Systems*, pp524–529, 1995.

[13] Kaneko, M., N. Kanayama, and T. Tsuji: 3D Active Antenna for contact sensing, *Proc. of the 1995 IEEE Int. Conf. on Robotics and Automation*, pp1113–1118, 1995.

[14] Kaneko, M., N. Kanayama, and T. Tsuji: Experimental Approach on Artificial Active Antenna, *Fourth Int. Symp. on Experimental Robotics*, pp141–146, 1955.

[15] Ueno, N., M. Kaneko: Dynamic Active Antenna — A principle of Dynamic Sensing, *Proc. of the 1994 IEEE Int. Conf. on Robotics and Automation*, pp1784–1790, 1994.

[16] Ueno, N., M. Kaneko: On A New Contact Sensing Strategy for Dynamic Active Antenna, *Proc. of the 1995 IEEE Int. Conf. on Robotics and Automation*, pp1120–1125, 1995.

[17] Kaneko, M., N. Kanayama, and T. Tsuji: Vision Based Active Antenna — Basic Considerations on Two-Points Detecting Method, *Proc. of the 1996 IEEE/RSJ Int. Conf. on Intelligent Robots and Systems* (To appear).